12th IMEKO TC4 International Symposium
Electrical Measurements and Instrumentation
September 25–27, 2002, Zagreb, Croatia

IDENTIFICATION OF ADC ERROR MODEL BY TESTING OF THE CHOSEN CODE BINS

Domenico Grimaldi[*)]*,Linus Michaeli*[**)]*,Peter Michalko*[**)]*,*

[*)]Department of Electronics, Informatics and Computer Science
University of Calabria, Arcavacata di Rende (CS), Italy
[**)]Department of Electronics and Telecommunications,
Technical University of Košice, Park Komenského 13, SK-04120 Košice, Slovakia

Abstract – Modelling of ADC allows to utilize testing of selected parameters for determination of its error model over whole operating range. While the integrating ADC model is characterised by polynomial shape of integral nonlinearity, the successive approximation ADCs are characterised by periodical appearance of significant values of differential nonlinearities related with each code bit. Unified behavioural error model cover wide scale of possible structures. The vicinity of tested integral nonlinearities with the modelled shape is shown on the base of the experimental results for two representatives of ADCs. The impact of the model parameter selection on the model accuracy is being studied in the paper. Those outcomes allow to choose the optimal fast testing method.

Keywords: Analog to Digital Converters, Modelling, Calibration.

1. INTRODUCTION

The character of the ADC uncertainties described by differential or integral nonlinerities (*DNL*(*k*), *INL*(*k*)) as a function of the ADC code bin k depends mainly on the architecture of utilized ADC. The generalized functional error characteristic which could be used for calculation of other metrological parameters are integral and differential nonlinearities.

Architectures of integrating ADCs (e.g. dual, multislope, or voltage – frequency) are basically formed by (i) an analog signal processing section, an integrator and a comparator and (ii) quantizing section represented by counter. Here the preprocessing section involves main nonlinearity in the final function comparing with the nonlinearities of quantisation section, moreover its character is continuous. In general, the integral nonlinearity of an ADC integrating could be modelled as a polynomial function of the code bin *k* [1]

$$INL(k) = A_0 + A_1 k + A_2 k^2 + ..A_L k^L \qquad (1)$$

The impact of the coefficients A_i of order higher than 4 is generally negligible for modern hardware components. First two components of the polynom covers the offset and gain error.

The main error sources in locating of the code transition levels $T(k)$ of a successive approximation ADC are the comparator and DAC in the feedback. Dominant feature of the functional error characteristic of DAC is linked with dismatching of the binary multiplied weights. The differences to the ideally doubled values cause the shift in the transition levels $T(k)$ inherent to the each bit k_i for $i \in (1,..N)$. Let consider $\Delta T(k)$ the total error contribution to the real transition code level $T_{real}(k) = Q.k + \Delta T(k)$, where Q is code bin width.

The value $\Delta T(k)$ taking in account the weight mismatching depends upon superposition principle on single bit contribution multipling it by k_i=0 or 1 from the output code bine k equal to $\Delta T(k) = \sum_{i=1}^{N} \Delta T_i k_i$. In particular, it will be only distinct N error effects on the ADC output, each one arising along the scale with the own periodicity. Hence, the ADC error presents different N periodicities along the scale, each related to the periodicity of a single bit k_i in the binary code [1], [6], [8].

These independent periodical effects have been modeled through a multiperiodical model for differential nonlinearity. Under this consideration, the differential nonlinearity has only N distinct values $DNL_O(i)$, each one arising correspondingly to the code bin $k=j.2^i+2^{i-1}$ for each bin position i=1,..N and for j=0,...$2^N/2^{i-1}$. Characteristic values of $DNL_O(i)$ related to each bit i emerges correspondingly to the negative derivation of the Rademacher function RAD(i,k)=sign[sin($2^i.\pi.k/2^N$) of the order i for the code bin k. The $DNL_O(i)$ function could expressed by the formula based on the difference of the Rademacher functions between code bins (k+1) and k.

$$\Delta RAD(i,k) = \begin{cases} 1 & if\ [RAD(i,k) - RAD(i,k-1)] \le 0 \\ 0 & if\ [RAD(i,k) - RAD(i,k-1)] > 0 \end{cases}$$
$$DNL_m(k) = \sum_{i=1}^{N} DNL_O(i) \Delta RAD(i,k) \qquad (2)$$

In this way, all the *DNL* values are estimated with only N experimental values (i.e. $2N$ measurements of code transition levels). In order to increase the accuracy in the determination of $DNL_O(i)$, the number of measured

differential nonlinearities belonging to the same bit position i should be large. The maximum accuracy of the model is achieved when all the homologous code bins are taken into account. The $DNL_O(i)$ is determined by mean value according to formulae

$$DNL_O(i) = \frac{\sum_{j=1}^{2^{N-i}} DNL(k)}{2^{N-i}} \quad \text{for} \quad k = 2^i.j + 2^{i-1} \qquad (3)$$

In general, the modelled values $DNL_O(i)$ increase with higher bit weights i in the output code k. It means that the modern SAR ADC posses the dominant values of the differential nonlinearity $DNL_O(1)$ in the middle of full scale (FS), lower $DNL_O(2)$ in the first and third quarter of FS. Further significant differential nonlinearity $DNL_O(3)$ occurs in code bins represented by odd octets of FS $\left(1/8, 3/8, 5/8, 7/8\right)2^N$. In general, the measured $DNL(k)$ values in code bins $k=(2^i.j+2^{i-1})$ for the same bit i positive change and any j are stochastic with mean value equal $DNL_O(i)$.

The highest number of multiperiodically modelled characteristic components $DNL_O(i)$ is determined by value I, representing upper limit of $i \le I$.

The modelled integral nonlinearity could by obtain by integration of the modelled values of the differential nonlinearity.

$$INL_m(k) = \sum_{l=1}^{k} DNL_m(l) \qquad (4)$$

2. UNIFIED ADC ERROR MODEL

The improvement in the technology of the SAR ADC production suppresses the multiperiodical error. Reduced integral nonlinearity caused by multiperiodical features of *DNL* increases the impact of the integral nonlinearity of analog components at the ADC input, like amplifier, multiplexer, reference voltage source etc. Highlighted main components properties in the SAR ADC error model could be expressed as one dimensional image in the code k domain.

This image consist of two components:

a) Low code frequency component (LCF) represented by polynomial approximation ${}^{\mathrm{LCF}}INL_m(k)$ of error caused by analog error components.

b) High code frequency component (HCF) ${}^{\mathrm{HCF}}INL_m(k)$ caused by multiperiodical occurrence of the modelled values of $DNL_m(k)$.

The modelled shape of the integral nonlinearity using both components is as follows

$$INL_m(k) = {}^{LCF}INL_m(k) + \sum_{l=0}^{k} DNL_m(l) \qquad (5)$$

Without high code frequency component remaining LCF integral nonlinearity component ${}^{\mathrm{LCF}}INL_{\mathrm{m}}(k)$ is a polynomial function. The LCF integral nonlinearity component ${}^{\mathrm{LCF}}INL_{\mathrm{m}}(k)$ covers the discrepancy in the periodical properties of the $DNL_m(k)$ caused by effects omitted in the deduction of SAR ADC model.

3. IDENTIFICATION OF ERROR MODEL PARAMETERS

The error modelling of analog to digital converters is aimed on two main objectives:

To allow users the description of the integral nonlinearity by a mathematical expression with the reduced number of identified parameters. The final error model represents a compression of 2^N values of measured nonlinearities into the few parameters of error model. Those parameters are coefficients of polynom approximating the ${}^{\mathrm{LCF}}INL_{\mathrm{m}}(k)$ component and the set of significant differential nonlinearities $DNL_O(i)$ i$\in\langle 1,I\rangle$, determining the high code frequency component.

To reduce time for ADC testing using measurement of the selected nonlinearity parameters in the crucial points of the FS range. Testing of ADC in the selected codes by static method [2], [6] or histogram testing by saw-tooth voltage with small amplitude [5], [6] are the possible ways how to reduce extremely long testing time caused by measurement of $INL(k)$ for each transient code level.

The estimation of high and low code frequency components from the measured values $INL(k)$ is being performed in successive steps. The order of the approximation steps is mutually replaceable. Both approaches determine the accuracy in the identification of error model parameters. The approximation algorithm estimating low code frequency is another feature determing the modelling accuracy.

4. APPROXIMATION OF MODEL COMPONENTS

The unified ADC error model was approved by the real measured data. The tested integral nonlinearity function has been acquired for two representatives of ADC with analog input processing unit represented by buffering amplifier and multiplexer. The tested ADC representation is as follows:

Data acquisition board Lab 1200 by National Instruments.

ADC converting unit embedded on ADuC 12 microcontroller.

The integral nonlinearity was measured by static test method. The testing voltage was generated by an integrator controlled from the output of PC comparing ADC output with measured code bin k. trolled by GP-IB. The precision of the multimeter connected at the input of ADC under test measures via GP-IB real transient code level $T(k)$. The multimeter ensures the required ADC testing uncertainty.

The first approximation approach based on the initial estimation of low code frequency component of ${}^{\mathrm{LCF}}INL_{\mathrm{m}}(k)$ utilise the least-squares fitting of approximation polynom. The residual function of the integral nonlinearity function $INL_{res}(k)= INL(k) - {}^{\mathrm{LCF}}INL_{\mathrm{m}}(k)$ is successively used for estimation of high code frequency component represented by $DNL_{\mathrm{m}}(k)$, where the values of differential nonlinearities are determined by the expression $DNL(k)= INL_{res}(k)-INL_{res}(k\text{-}1)$. The averaged value of $DNL(k)$ according to formulae (3) determines the modelled values of $DNL_{\mathrm{O}}(i)$.

The results of model identification for different number of the modelled high frequency components and coefficients

of accuracy of such approximation by the best fitted polynom by least mean squared (LMS) value algorithm for DAQ Lab 1200 are shown on Fig.1.

The modelling accuracy was assessed by standard deviation σ_{app} between measured $INL(k)$ and modelled $INL_m(k)$ function according to formula

$$\sigma_{app} = \sqrt{\frac{\sum_{k=1}^{N-1}(INL(k) - INL_m(k))^2}{N-1}} \qquad (6)$$

The opposite approximation approach is based on the initial determination of the modelled value of differential nonlinearity from the difference between coupled values of measured integral nonlinearities. The averaged value $DNL_O(i)$ by (3) determines the high frequency component of integral nonlinearity ${}^{HCF}INL_m(k)$. This value is successively subtracted form the measured shape. The residual function of the $INL_{res}(k)$ = $INL(k)$ - ${}^{HCF}INL_m(k)$ is being used for approximation of the low code frequency component ${}^{LCF}INL_m(k)$.

The experimental results showed that the first approach determines low code frequency component by the optimal regression polynom. The additive high frequency component is being represented by the mulitperiodical properties of the $DNL_m(k)$. This estimation could be taken as the reference close to the ideal splitting both components.

The second approach utilise for the estimation the residual shape of the integral nonlinearity $INL_{res}(k)$, which is more smoothed comparing the measured function $INL(k)$. The values for estimation of ${}^{LCF}INL_m(k)$ in the nodal points are redeemed from high code frequency components. The remaining casual components are caused by uncertainty of the $INL(k)$ measurement. This fact allows to assess low code frequency component ${}^{LCF}INL_m(k)$ by the fast algorithms like Lagrange or spline approximations. The uncertainty of the measurement could be rejected using mean value for code window around the nodal points.

Authors studied various approximation algorithms for identification parameters of polynom (1). Every methods is differently sensitive on the uncertainty in the measurement of $INL(k)$ in the approximating nodes.

The approximation taken as a reference is the approximation, where the polynom is determinate by LMS algorithm. The resulting polynom represents optimal low code frequency component ${}^{LCF}INL_m(k)$. The sum of low and high code frequency component represents final shape of modelled $INL_m(k)$. The Fig.2 shows the impact of the high code frequency component modelling on the accuracy of final model represented by both components. The accuracy of the high frequency modelling is expressed by the maximal number I of modelled $DNL_O(i)$ of the unified ADC error model.

a) b)

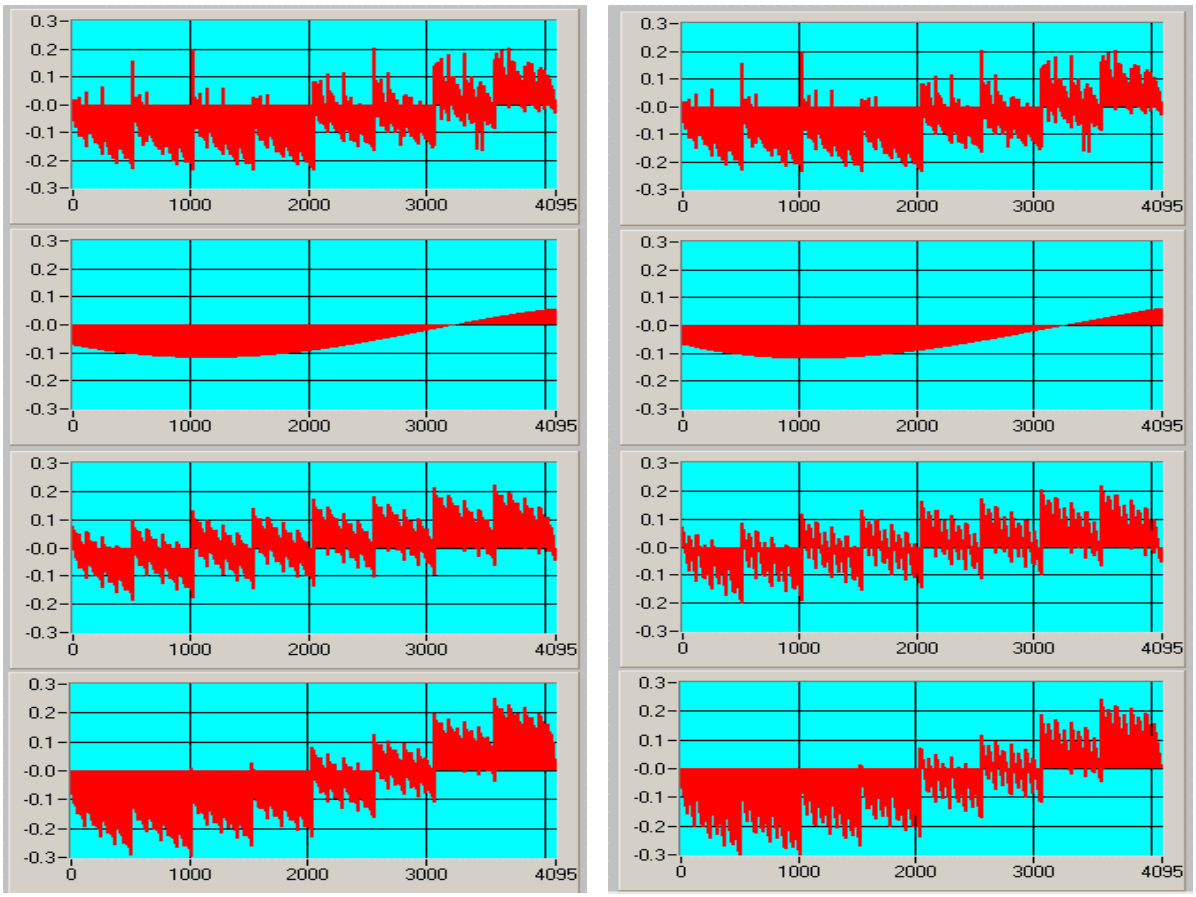

Fig. 1. Measured and modelled low and high code frequency components and final unified error model: a) Modelled deepness of high frequency components I= 4 and order of LCF polynom is k=3; b) Modelled deepness of high frequency components I= 5 and order of LCF polynom is k=4

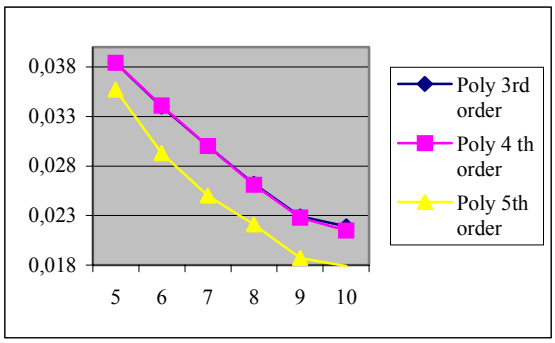

Fig. 2. Relation between σ_{app} and maximal number I of modelled DNL_m.

The approximation by Lagrange polynom represents a faster algorithm for the approximation of low code frequency component from the residual integral nonlinearity function $INL_{res}(k)$. The well-known weakness of the Lagrange polynomial approximation is its sensitivity on the uncertainty in determination of approximated values in the nodes of experimental data. Calculating mean value around the code bine of the approximated node enhanced the accuracy of the residual integral nonlinearity. The Fig. 3 shows results obtained for Lagrange approximation using window of W results for estimating value in the nodes.

The Fig. 2 shows the impact of the high code frequency component modelling on the accuracy of final model represented by both components.

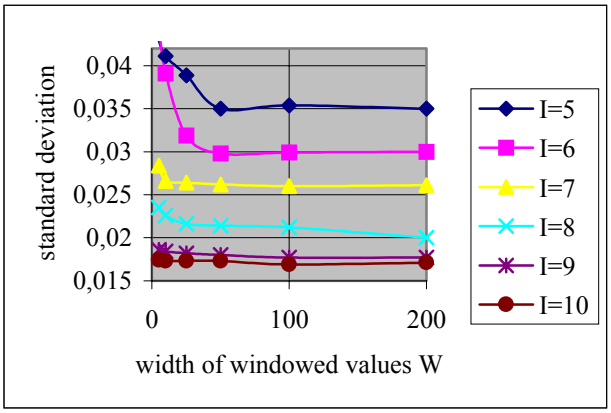

Fig. 3. Relation between σ_{app} and number of windowed values W around the approximation nodes by Lagrange polynom for I modelled $DNL_O(i)$.

The accuracy final ADC model using LCF approximation by Lagrange polynom as a function of the deepness of HCF modelling expressed by I of multiperiodical components is shown on Fig.4. The standard deviation between modelled and measured nonlinearity decrease monotonously until I=9.

Other type of studied approximation method was the spline interpolation.

Taken points for low code frequency component has been equidistant. The comparison of the uncertainty among approximation for different position shows the situation that the optimal results has been achieved for equidistant sampling of the characteristic. The highest impact on the accuracy has the samples on both margins of the full scale.

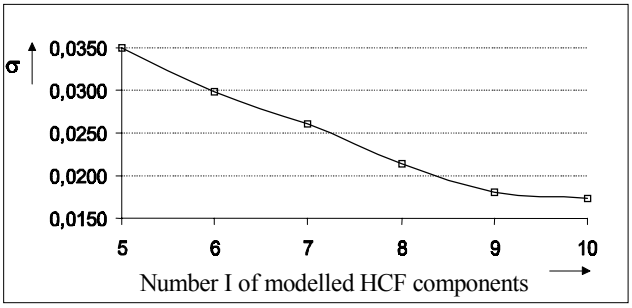

Fig. 4. The impact of approximation uncertainty by Lagrange approximation for different deepness I of modelling of multiperiodical component.

Fig. 5 shows the approximation the results of the approximation for ADC embedded on the microcontroller AduC12.

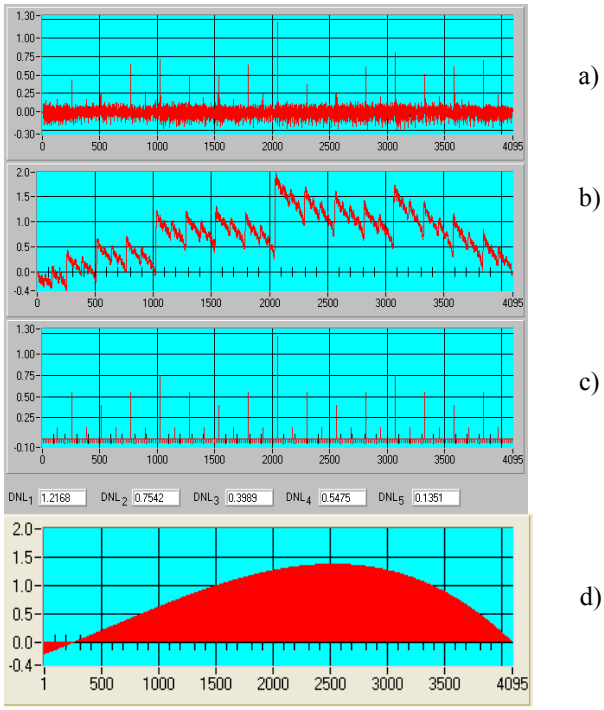

Fig. 5. Measured DNL (a) and INL (b) of ADC embedded on the ADuC microcontroller. Modelled $DNL_m(k)$ (c) and ${}^{LCF}INL_m(k)$ (d)

The measurement performed on the both representants of ADC with resolution of 12 bit shows the notable aberration of the $DNL_m(k)$ function to the ideal multiperiodical behaviour presented at the beginning. This difference is more notable in the case of the ADC embedded on DAQ board Lab 1200. In addition to the basic multiperiodic properties occurs alternation of two values around the mean value $DNL_O(i)$. This fact could be caused by inherent circuital properties non considered in the model [1], [6], [8] or caused by the trimming technological step in the ADC production. Progress in the technology and unknown circuit layout prefer the modelling approaches extrapolating model

parameters from the regularities in the final measured behaviours. This approach is notable in the paper [9] were the authors supposed besides the sum mismatching values ΔT_i related to each bit of output code the contribution of the higher order errors. The non-linear error contribution of second order is represented by the simultaneous presence of code bits k_i,k_j - ΔT_{ij} . The third order non-linear components represents the error contribution related with code bits k_i,k_j,k_k - ΔT_{ijk} and soon.

Taking in the account the properties of differential non-linearities shown on the Fig. 6 authors suggested an easier correction algorithm. This one improves the modelling accuracy for the modelled value by simple alternation of deviation from the mean value $DNL_m(k) = DNL_O(i)\Delta\mathrm{RAD}(k,i) + \delta DNL_O(i)(-1)^j$ where j is related with k by $k=j.2^i+2^{i-1}$.

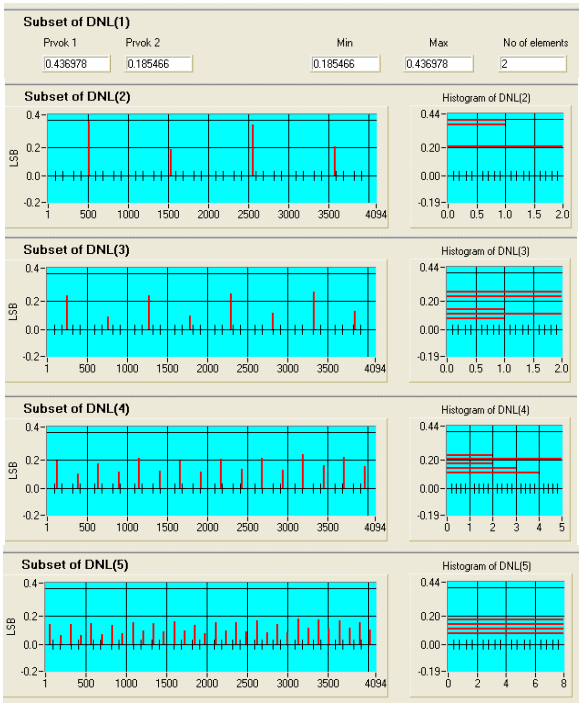

Fig. 6. Additional periodicity of the odd and event components of $DNL_O(i)$ of DAQ Lab 1200 NI.

5. IDENTIFICATION OF THE MODEL COMPONENTS BY FAST TESTING METHODS

As mentioned before the unified error model is suitable for approximation of real error characteristic by the measurement of dominant model parameters using fast testing methods. One known possibility of *DNL* testing is the utilisation of a triangular voltage with small-amplitude [6]. Experimental results performed by this method for two representative of digital instruments with high accuracy are published in the [5]. Described fast static testing method is appropriated for testing of the main differential nonlinearities $DNL_O(i)$.

The low code frequency ${}^{\mathrm{LCF}}INL_m(k)$ could be determined by the evaluation of FFT spectra from the ADC output stimulated by harmonic testing signal. The spectral components are distorted by the shape of the polynom ${}^{\mathrm{LCF}}INL_m(k)$. The FFT spectral components at the multiplies of basic testing frequency f_T generated with testing generator with low distortion (Stanford Research). Input signal is $X_0\sin(2\pi f_T t)$. The relation between four basic components in the FFT spectra $(K(0),K(f_T),K(2f_T),K(3f_T))$ and coefficients (A_0, A_1, A_2, A_3) in the 3rd order polynom are expressed [8] by

$$A_0 = -(K(0) - K(2.f_T)) \quad A_1 = \frac{(K(f_T) - 3.K(3.f_T))Q}{X_0}$$
$$A_2 = \frac{2.K(2.f_T)Q^2}{X_0^2} \qquad A_2 = \frac{4.K(3.f_T)Q^3}{X_0^3} \tag{7}$$

Here Q represents the average code bin width.

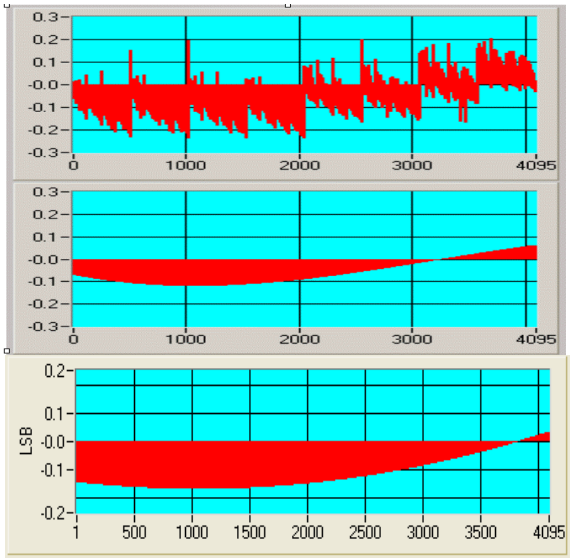

Fig. 7. Measured INL(k) (a.) modelled (b) and by the FFT assessed components (c) of ${}^{\mathrm{LCF}}INL_m(k)$ for DAQ Lab 1200 NI.

The efficiency of the ${}^{\mathrm{LCF}}INL_m(k)$ coefficient identification was assessed using FFT spectrum by the software simulation. The model of real ADC characteristic was obtained adding to the ideal values of the transient voltages $T(k)$ measured values of $INL(k)$ of the DAQ Lab 1200. The conversion of ideal harmonic function $X_0\sin(2\pi f_T t_S i/2^N)$ by the ADC software model was performed for ideally coherent sampling $f_T t_S i/2^N$ by the 2^{15} samples. Fig. 7 shows the measured $INL(k)$ containing low code frequency component ${}^{\mathrm{LCF}}INL_m(k)$ and by the FFT assessed their shape.

6. CONCLUSIONS

Experiments with the two representants of 12 bit ADC shows that the ADC error model composed of low and high code frequency allow cover effects of dominant error sources inherent for large scale of ADC structures. Those errors are mismatch in the ADC weighting network and offset, gain and nonlinear distortion of the analog block transfer characteristics. Moreover, the approach based on the signal processing of the one dimensional images could be spread on the other regular phenomena in the shape of the nonlinearity components.

The various fast approximation algorithms allow to model the low code frequency component. Among them the spline and Lagrange approximation is represented by trade of computing complexity and modelling accuracy. The averaged values across a window of the measured data allow to reduce uncertainty in the approximation nodes.

Experiments show the possibility to use the histogramme test with the small-amplitude waves for estimatind of the high code frequency component. Simulation experiments shows the possibility of FFT test for estimation of the polynom coefficient modelling the low code frequency component. The only problem in the practical implementation with non coherent sampling will be the impact of windowing on the accuracy of calculation of single spectral components.

ACKNOWLEDGMENT

This work has been supported by the Slovak Research Agency VEGA project No. 1/9030/02.

REFERENCES

[1] Arpaia, P., Daponte, P., Michaeli, L.: "The influence of the architecture on ADC modelling", *IEEE Trans.on Instrumentation and Measurement*, Vol. 48, No. 5, pp. 956-967, October 1999, ISSN 0018-9456

[2] IEEE Std. 1057 - 1994, "IEEE Standard for Digitizing Waveform Recorders", *Institute of Electrical and Electronics Engineers*, Inc. New York, USA 1994

[3] Michaeli, L.: "Fast Dynamic Methods of the Systematic Error Autocorrection", *Proc.of the 5-th International Symposium on Electrical Measuring Instruments for Low and Medium Frequencies*, IMEKO TC-4, Vienna, April 1992, pp. 247-249.

[4] Brigati, S., Liberali, V., Maloberti, F.: "Precision behavioural modelling of circuit components for data converters", *Proc. of IEE Conference on "Advanced A-D and D-A conversion tecniques and their applications"*, Cambridge (UK), 6-8 July, pp. 110-115, 1994.

[5] Alegria, F., Arpaia, P., Serra, A. Cruz, Daponte, P.,: "An ADC histogram test based on small-amplitude waves", *MEASUREMENT*, VOL. 27 (2001), No. 4, ISSN 0263-2241

[6] Michaeli, L.: "The Fast method for correction of systematic errors of ADC histogram measurements", *Acta X IMEKO World Congress*, Vol. 5, pp. 40-47, Praha 1986.

[7] Mikulik, P, Šaliga, J.: "Volterra Filtration Technique for IADC Error Correction, based on an a-priori Error Model", *Proc. of IEEE IMTC2001 Conference*, Budapest, Hungary, Vol. 3, pp. 1672-1677.

[8] Vargha, B., Zoltan, I: "Calibration Algorithm for Current – output R-2R Ladders", *IEEE Trans. on Instrumentation and Measurement*, Vol. 50, No. 5, pp. 1216-1220, October 2001, ISSN 0018-9456

[9] Vargha, B., Shoukens, J., Rolain, Y.: "Non-linear Model Based Calibration of A/D Converters", *Proceedings 6th Euro Workshop on ADC Modelling nad Testing*, Sept. 2001.

[10] Mirri, D. G. Iuculano, F. Filicori, G. Pasini, G. Vannini, "Modeling of Non Ideal Dynamic Charasteristics in S/H-ADC Devices", *Proceedings of IMTC'95*, Waltham, Mass. USA April 22-26. 1995, p.27-32.

[10] Kocur, D.,Hendel, I.: "Adaptive Microstatistic Volterra Filters", *J. Electrical Engineering*, 49 (1998), No. 9-10, pp. 225-231.

[11] Smiesko, V., Kováč, K., Kazička, R.: "VXI-bus as a Tool for Dynamic Testing", *Proc. Int. Conference CATE 93*, Brno 1993, pp. 283-287.

[12] Vrba, R.: "Testing and Analysing of the ASI Bus System,Advances in Intelligent Systems", *IOS Press.* 1997, pp. 51-55.

Authors: Assoc.Prof.Domenico Grimaldi, Department of Electronics, Informatics and Compouter Science University of Calabria, I-87100 Arcavacata di Rende (CS), Italy +39984494712, grimaldi@deis.unical.it Prof.Linus Michaeli,PhD ,Ing.Peter Michalko,Department of Electronics and Telecommunications, Technical University of Košice, Park Komenského 13, SK-04120 Košice,+421556022857, Linus.Michaeli@tuke.sk, Peter.Michalko@tuke.sk